Marine Biology 106, 91–101 (1990)

Marine Biology
International Journal on Life in Oceans and Coastal Waters

Morphogenesis of opal teeth in calanoid copepods

C. B. Miller [1], D. M. Nelson [1], C. Weiss [2,*] and A. H. Soeldner [2]

[1] College of Oceanography, Oregon State University, Corvallis, Oregon 97331, USA
[2] Electron Microscopy Service, Oregon State University, Corvallis, Oregon 97331, USA

Date of final manuscript acceptance: April 2, 1990. Communicated by M. G. Hadfield, Honolulu

Abstract. Opal teeth of calanoid copepods develop early in the premolt phase of the molt cycle. They form in the apolysis space beneath the old tooth row on the mandibular gnathobase. We examined stages of tooth formation in *Neocalanus* spp. and *Calanus pacificus*. Apolysis occurs early in the distal gnathobase, then several epidermal cell types participate sequentially in formation of new teeth. Fibrous molds in the shapes of the new teeth are extruded onto the epidermal surface, then additional materials, probably proteinaceous, are secreted into them. Tooth molds next are linked to a gland in the proximal part of the gnathobase by ducts of an unusual type, "lamellar-walled ducts." Silicification follows, apparently using highly osmiophilic material supplied by the proximal gland. Opal is laid down at the outer periphery of the mold then thickens toward the attachment of the mold to newly formed chitin at its base. During apolysis the epidermal cells move proximally without breaking ducts that connect small dermal glands with pores in the sides of the opal teeth. The molds for the new teeth form surrounding these ducts, and new pores result. The glands are like the ciliary exocrine glands seen in other Crustacea, with the duct deriving from fusion of the axonemes of a cilium. Presumably the glands secrete a substance into food newly broken by the teeth. This could be a toxin or a digestive enzyme.

Introduction

Calanoid copepods bear cuspate, opal teeth on the chewing surfaces of the mandibular gnathobases or jaws (Beklemishev 1954, 1959). Sullivan et al. (1975) suggested that the hardness of these teeth evolved as a match for that of opal-covered food particles such as diatoms. They described the external appearance of the teeth in several species, and Miller et al. (1980) showed that *Acartia tonsa* obtains silica for teeth directly from the water; a dietary source is not required. Siliceous teeth formed by *A. tonsa* in media of low silicic acid concentration are weak and crumbly. We describe here the morphogenesis of the opal teeth in the family Calanidae based on observations by differential interference contrast microscopy ("Nomarski", DIC) of whole jaws and transmission electron microscopy (TEM) of thin sections. The ultrastructural results, in conjunction with the DIC information, permit description of the main sequence of events. In addition, we report x-ray fluorescence (microprobe) and electron diffraction studies of tooth composition and internal structure, which further confirm that they consist of opal, as opposed to a crystalline silicate.

* Present address: P.O Box 32, Petersburg, Alaska 99833, USA

Materials and methods

Differential interference contrast microscopy

Because of their large size, fourth copepodites (C4) of *Neocalanus plumchrus* and *N. cristatus* were used for the micrographs (Figs. 1–3) shown here (C5 of these species do not form new teeth, and the mandible of the adult is toothless). Specimens (preserved with 5 to 7% formaldehyde) were sorted from ordinary net samples collected in the northern Sea of Japan and southern Oyashio region on various dates. Using dissecting needles and a stereomicroscope, the entire mandible was removed by (1) breaking away the labrum which covers the gnathobases ventrally, (2) inserting a needle at the attachment of the mandible to the ventral exoskeleton, and (3) pulling gently. The arthrodial membrane that attaches the proximal end of the gnathobase to the body tears easily and the mandible was thus separated from the body. Whole mandibles were mounted in glycerine-water (1 : 1) and pressed under coverslips for examination and photography using 20 ×, 40 ×, and 100 × objectives of a Nikon DIC microscope and camera system.

Transmission electron microscopy

Fifth copepodites of *Calanus pacificus* Brodsky were sorted alive from plankton collected 2 to 10 nautical miles off either Newport, Oregon (various dates in 1979–1980), or La Jolla, California (many dates in 1980–1981), USA. Sorted C5 were fixed in 4% glutaraldehyde in seawater. Keeping the stock of specimens in cold buffer,

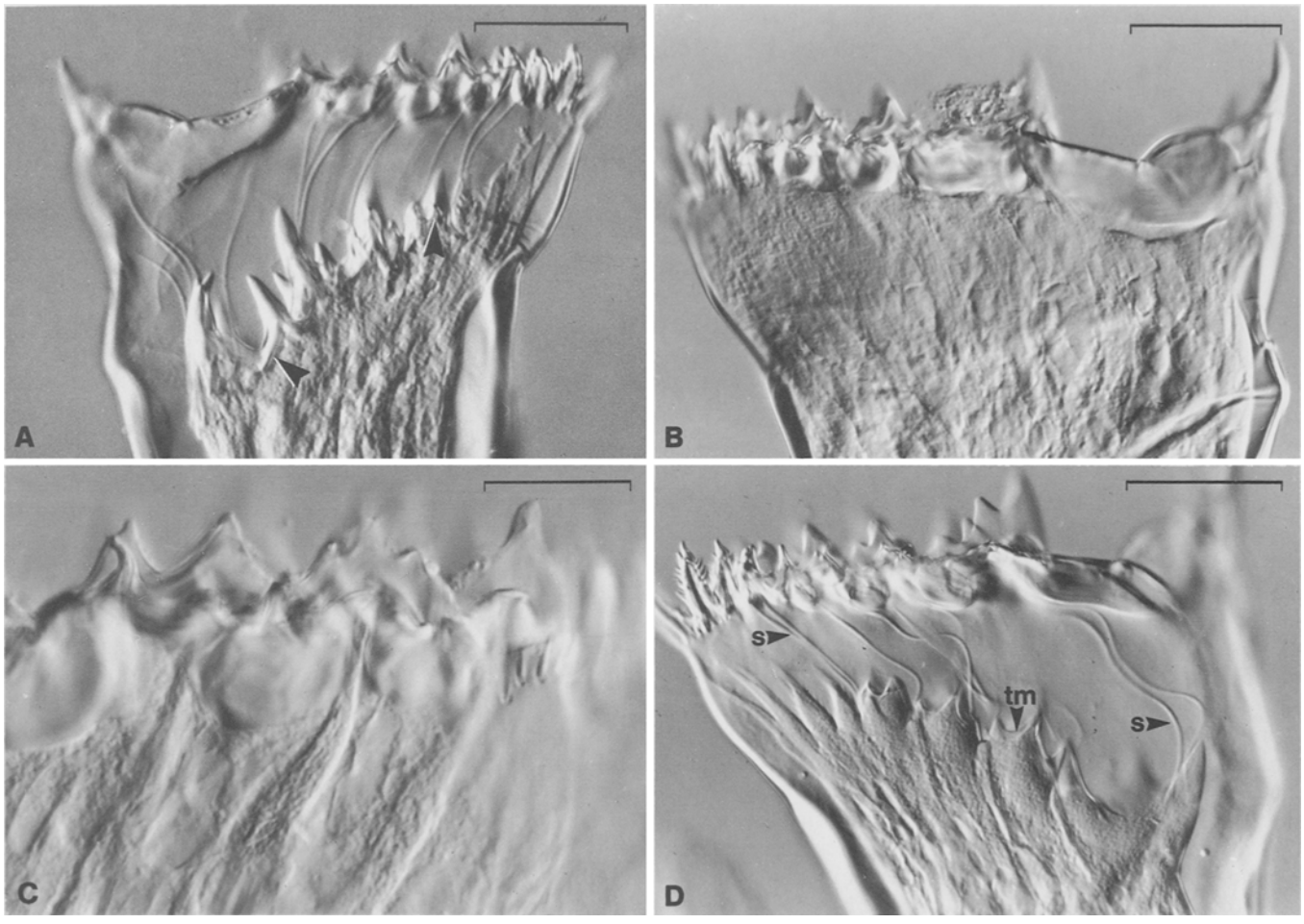

Fig. 1. *Neocalanus plumchrus* (A, C) and *N. cristatus* (B, D). (A) Jaw in process of forming new teeth in apolysis space below old tooth row; tooth molds are fully extruded onto surface of epidermis (arrowed) and have cuspate shape of tooth (scale bar = 80 μm). (B) Jaw at interphase of molt cycle; epidermis is little differentiated under tooth row (scale bar = 65 μm). (C) Jaw just prior to apolysis; epidermis beneath old teeth takes on a distinctly striated appearance (scale bar = 30 μm). (D) Jaw after apolysis at an early stage of extrusion of tooth molds from terminal ends of epidermal cells, showing (arrowed) "salivary" ducts (s) passing through tooth molds (tm), apolysis space, and old exoskeleton (scale bar = 70 μm)

jaws were dissected one by one as described in the preceding subsection, classified with respect to tooth development phase, and stored individually in numbered shell vials of cold buffer. Using Pasteur pipettes, the jaws were transferred through an alcohol series to a saturated solution of uranyl acetate in 70% ethanol and left for 2 h. They then were taken back through the alcohol series to buffer, then through an acetone series to 100% acetone, and finally to Spurr's embedding formula without hardener. After soaking overnight in Spurr's medium, they were transferred to Spurr's with hardener and aligned in numbered molds for hardening. Ultrathin sectioning was done with a diamond knife, producing gold and silver interference colors. In some cases, roughly serial sections were obtained by collecting groups of sections on a series of grids. Sections on grids were stained with Reynold's lead citrate for 3 min. Grids were examined and photographed using a Phillips 300 TEM at various magnifications, mostly using 60 kV accelerating potential.

One scanning electron micrograph (Fig. 5A) is presented. It is of an air-dried, gold-paladium-coated mandibular gnathobase of *Neocalanus plumchrus*. Technical details for Fig. 5A are the same as for figures in Sullivan et al. (1975).

Microprobe analysis

Fifth copepodites of *Calanus pacificus* were collected off La Jolla in April 1981 and fixed with 4% glutaraldehyde, but not post-fixed with osmium. They were mounted in Spurr's medium and sectioned. Sections mounted on 180-mesh, carbon-coated nylon grids were examined with a Hitachi H500 scanning-transmission electron microscope equipped with an ORTEC, 7850S-455, Si(Li) energy-dispersive x-ray analyzer. This produces an approximate elemental analysis of elements with atomic weight ≥ 18 for spots as small as 100 nm diam within sections. Precise analysis requires the parallel study of standards closely matched in composition and thickness to the matter of interest; this was not done in the present study. The same microscope was used to produce electron diffraction images.

Results

Although the DIC study was of *Neocalanus* spp. and the TEM study was of *Calanus pacificus*, these genera are closely related members of the family Calanidae. Their processes of tooth formation are the same. DIC examination of *C. pacificus* reveals all the structures seen in the DIC micrographs from *Neocalanus* spp. We worked with the two genera because of availability and because the large *Neocalanus* spp. give large DIC images, while the smaller *C. pacificus* show several structures between

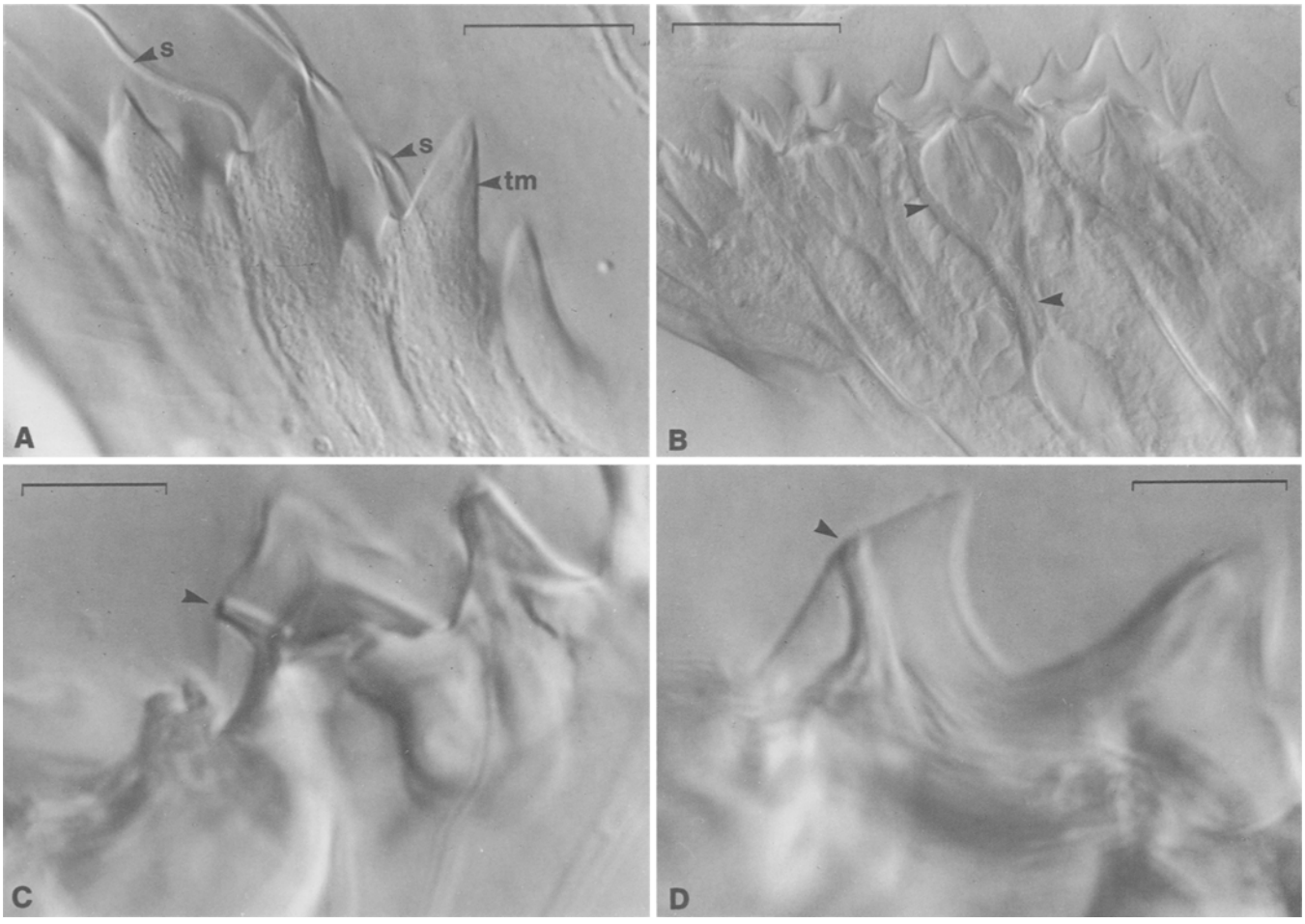

Fig. 2. *Neocalanus cristatus* (A, C, D) and *N. plumchrus* (B). (A) Detail of tooth molds of specimen in Fig. 1 D on different focal plane; abbreviations as in Fig. 1 D (scale bar = 40 μm). (B) New teeth forming, showing "Y" ducts (arrowed) attached at dorsal and ventral corners of several of tooth molds (scale bar = 40 μm). (C), (D) Examples of "salivary" ducts passing through cusps of central teeth; arrow indicates duct openings on teeth (scale bars = 10 μm)

TEM grid wires. A tooth-formation process similar to that described here probably operates in all of the calanoid copepods with siliceous teeth (Sullivan et al. 1975).

Morphogenetic sequence

The development sequence is illustrated by DIC micrographs; the ultrastructural details by TEM. New teeth form on the surface of the epidermis just below the line of old teeth (Fig. 1 A) in a space made by withdrawl of the epidermis from the exoskeleton (apolysis). Apolysis occurs only in this part of the gnathobase, after about seven-tenths of the molt cycle is complete, long before it occurs elsewhere in the body. Formation of the teeth involves a series of events in the distal ends of columnar epithelial cells, whose nuclei are located proximally in the shaft of the gnathobase.

In the interphase of the molt cycle (Drach and Tchernigovtzeff 1967), well before apolysis (Fig. 1 B), there is little differentiation visible by DIC. Tooth formation is initiated when distinct columnar structures appear beneath each of the heavy thickenings in the chitin supporting the old teeth (Fig. 1 C). The columns are separated from each other by striated or fibrous zones which extend from the most proximal part of the gnathobase to the inner surface of the exoskeleton just under the centers of the teeth. Apolysis follows, and a space of variable size (Fig. 1 D) opens between the chitin supporting the old teeth and the distal edge of the epithelium. A set of fine tubules traverses the apolysis space. Tubules run from the epithelium surface (Fig. 2 A) across the apolysis space, through the chitin under the base of the old teeth, and right through the opal substance of the old teeth. They open on the tooth surfaces (Fig. 2 C, D), well below the apices of the pointed cusps. Close inspection shows that every duct ends at a separate pore on a tooth surface, except for the ventral tooth where several ducts appear to share a common opening. Similar ducts and pores are present throughout the molt cycle. They are more readily seen after apolysis because the epithelium has slid proximally, leaving them exposed across the apolysis space.

In jaws only slightly advanced from the apolysis stage (Figs. 1 D and 2 A), a set of what we term "tooth molds" appears in the distal ends of epithelial cells, one on each

columnar structure below the old teeth. These become progressively longer, protruding more into the apolysis space, and more and more obviously acquiring cuspate forms characteristic of individual teeth (Fig. 1 A). The tubules traversing the apolysis space emerge into it through these tooth molds (Fig. 2 A).

Finally, silicification occurs. During this phase, each tooth mold is connected at its dorsal and ventral corners to branches of a Y-shaped duct (Fig. 2 B). The stem of each "Y" extends back to the proximal portion of the gnathobase (Fig. 3 A), and ducts from all the tooth molds are seen to connect there to a mass of glandular tissue. We suspect that unpolymerized silicic acid, possibly bound to a protein or other carrier molecule, is supplied by the gland and transferred to the mold through these ducts. Simultaneous with silicification, the surface of the jaw apart from the teeth proper begins to acquire birefringence (in phase-contrast) as the new chitin forms over the surface. Since the new, larger exoskeleton is contained within the smaller, old one, there are folds to accommodate the new surface. Folds are particularly obvious in the direction of the long axis of the jaw (Fig. 3 B).

Withdrawal of the jaws from the old exoskeleton is the first step in actual ecdysis; this occurs before the general opening of the suture between the pleurites and sternites along the anterior, ventro-lateral edge of the cephalosome. The new gnathobases meet above the old ones, just before this suture splits. After the copepod is out of the exuvium, it expands, presumably by water uptake as is the case in other Crustacea (Skinner 1985). The physiological mechanism of this uptake is presumably like that in *Homarus americanus* (Mykles 1980). During this phase, the hemocoele expands into the gnathobase as a distinctly visible space or sac. This hemocoele space is sharply defined against the anterior (concave) exoskeleton (Fig. 3 C), providing a good indicator of recent molting (postmolt phase). The distal epithelial cells during this phase may take the appearance of a taut, shrunken webbing extending from the teeth back to the isthmus section of the jaw. After some time, if food is available (Miller et al. 1984), the appearance of the mandible returns to the interphase condition. However, calanid copepodites preparing for a resting phase with abundant food available can grow dramatically and not lose the hemocoele outline in the jaw. It is retained in lipid-rich specimens from deep-dwelling, resting-stage populations. The presence of the hemocoele in the mandibular gnathobase can sometimes be used as a criterion for determining whether individuals are in a resting phase (Miller and Terazaki 1989).

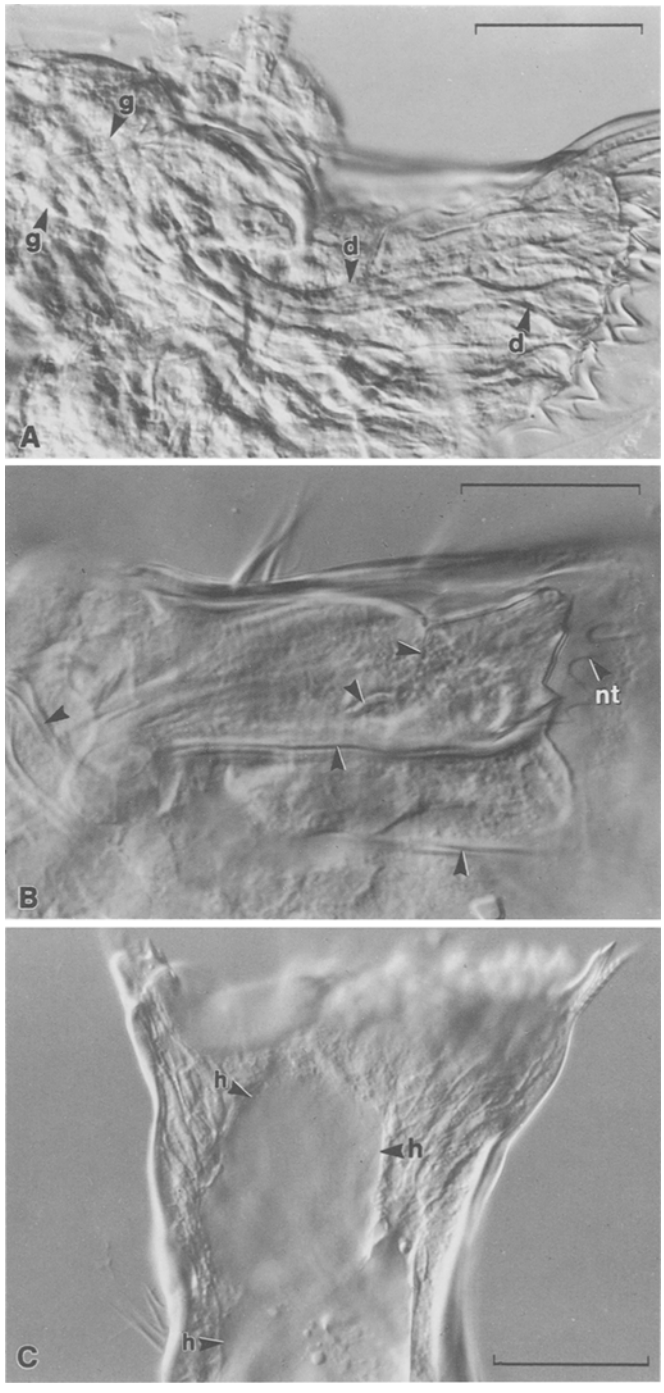

Fig. 3. *Neocalanus plumchrus* (A, B) and *N. cristatus* (C). (A) Jaw at silicification phase; tooth molds are connected to a gland (g) in base of the jaw by ducts (d) which bifurcate just proximal to tooth mold (scale bar = 80 μm). (B) Jaw in late premolt phase, showing a new tooth (nt); folds in new exoskeleton appear as double-interference stripes (unlabelled arrows) (scale bar = 40 μm). (C) Jaw in postmolt phase; extension of hemocoele (h) fills the anterior side (scale bar = 90 μm)

Ultrastructure of tooth morphogenesis

Tooth molds are formed in the distal ends of some epidermal cells just prior to and just after the local apolysis under the tooth row. At apolysis the molds are contained in epidermal cells (Fig. 4 A) and have become separated from the rest of the cytoplasm by a membrane. They contain an array of microtubules and some large, apparently empty vesicles. Tooth molds are extruded into the apolysis space, leaving a cavity in the cell below (Fig. 4 B). At the time of extrusion the microtubules in the molds are more distinct and arranged roughly parallel to the contours of the mold. We are not certain whether the mold-forming cell retreats from the surface at this point or takes on a new function.

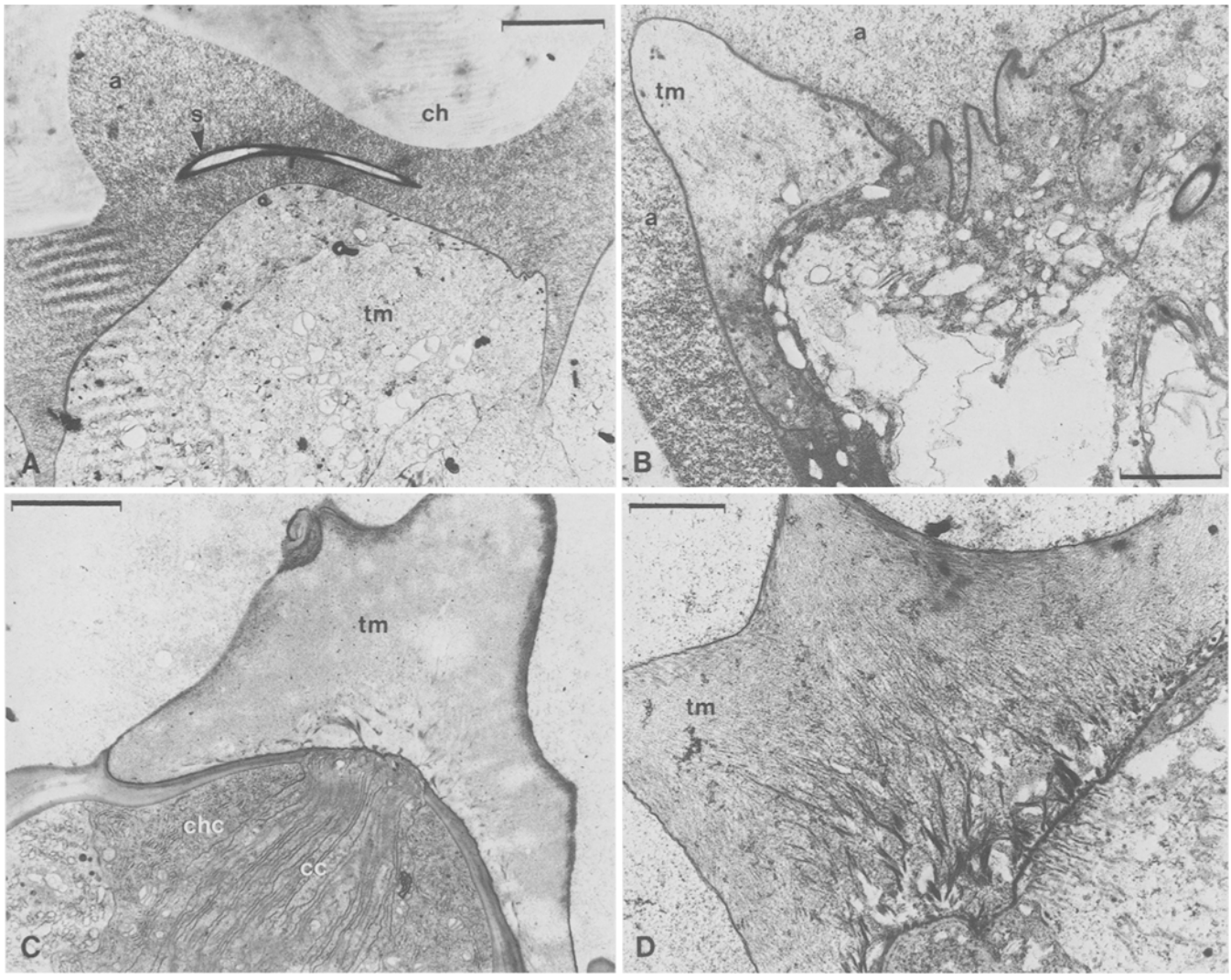

Fig. 4. *Calanus pacificus*. (A) Section parallel to tooth row of distal end of a mandibular gnathobase; a fluid-filled apolysis space (a) lies between chitin (ch) and ends of epidermal cells; a salivary duct (s) is in apolysis space; a tooth mold (tm) at initial stage of extrusion into apolysis space is visible within an epidermal cell; developmental stage is same as for Figs. 1 D and 2 A (scale bar = 4.0 μm). (B) Section parallel to tooth row, showing a tooth mold (tm) newly extruded into apolysis space; development stage is later than in Fig. 4 A (scale bar = 2.3 μm). (C) Section parallel to tooth row, showing connection of central cell (cc) to a tooth mold (tm); chitin-secreting cells (chc) have laid down some chitin; developmental stage just later than Fig. 4 B (scale bar = 3.5 μm). (D) Section parallel to tooth row, showing "fiber fountains" in a tooth mold (tm) (scale bar = 2.0 μm)

In the next phase, two epidermal cell types become associated with the proximal surfaces of the molds. One type is a "central" cell (Fig. 4 C), whose distal end attaches to the mold by a complex network of folded lamellae. The surfaces of these lamellae run proximal to distal in the cell, so that they appear as "ducts" in all section planes except transverse to the gnathobase (parallel to the tooth row). This is illustrated for a later phase in Fig. 7 A. Fiber density in the tooth molds increases greatly at this time, perhaps from material injected through the central cell lamellae. There appear to be "fiber fountains" (Fig. 4 D) entering the molds from the area of the central cell attachment, but also extending laterally. None of our micrographs shows masses of either rough or smooth endoplasmic reticulum in the distal portion of these cells to support material synthesis. There are, however, cell sectors proximally (Fig. 7 D) with copious rough endoplasmic reticulum (RER; a protein-secreting organelle), and these may be the proximal portions of central cells. Attachment of the central cells to the molds persists long into the silicification phase (Figs. 6 A, 7 A and 8 A), and we believe that there is a gap in the chitin beneath each tooth that never fills (Fig. 5 A; SEM of the chitin beneath a mature tooth).

The other epidermal cells abutting the tooth molds are chitin-deposition cells displaying ultrastructural appearance typical for Crustacea (Bocquet-Vendrine 1979, Doughtie and Ranga Rao 1979). They extend under the tooth molds from all sides, surrounding the attachment of the central cell. These cells deposit material beneath the mold in two phases. An electron-dense substance accumulates in surface invaginations on these cells

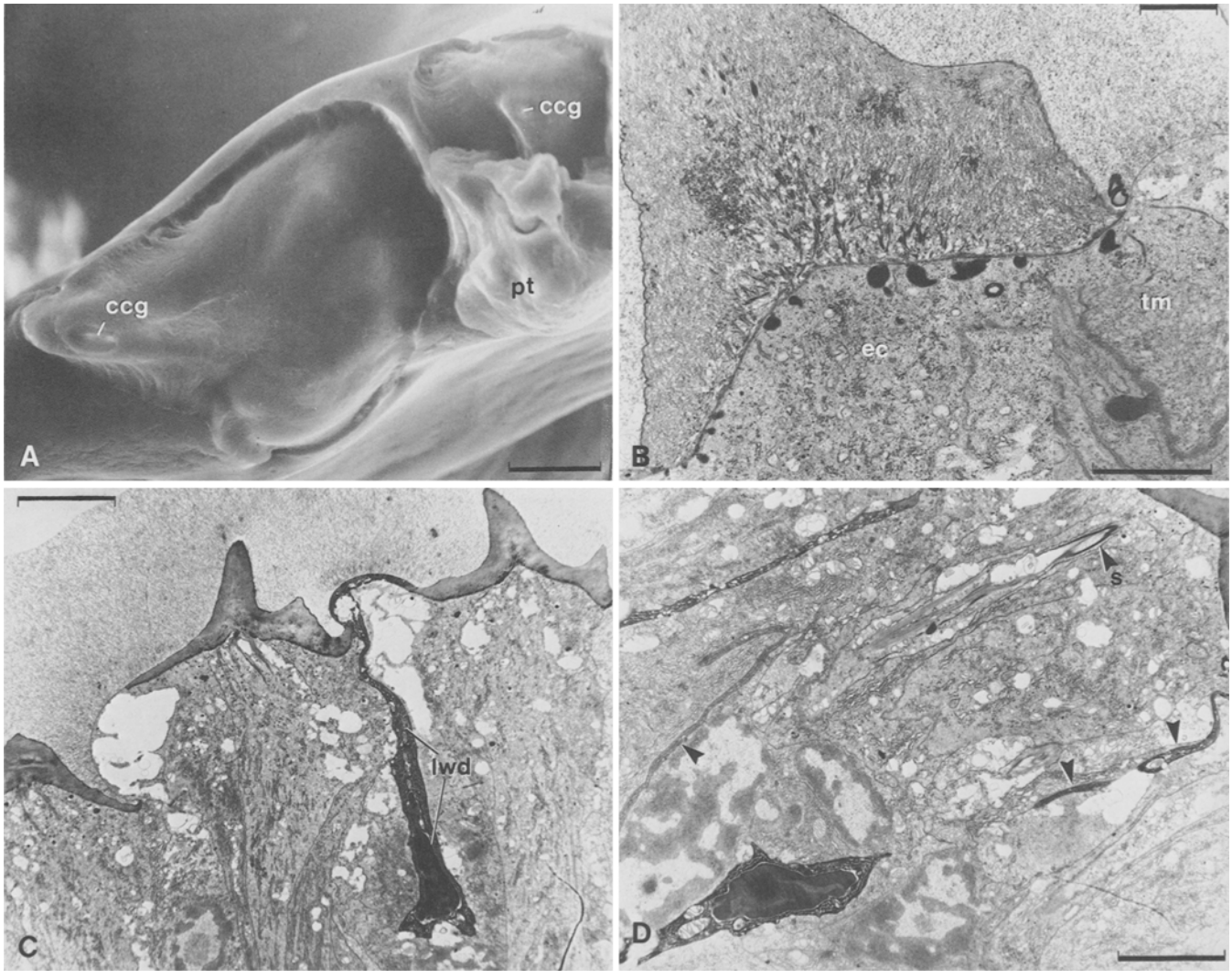

Fig. 5. *Neocalanus plumchrus,* fifth copepodite (A) and *Calanus pacificus* (B, C, D). (A) SEM picture of chitin surface beneath a siliceous tooth; central cell gaps (ccg) and a partial tooth (pt) are indicated (scale bar = 4.0 μm). (B) Section parallel to tooth row of an epidermal cell (ec) beneath a new tooth mold; electron-dense secretion accumulates in cell surface-invaginations next to tooth mold (scale bar = 2.0 μm); inset: example of secretion apparently being deposited between tooth mold (tm) and an epidermal cell (scale bar 1.0 μm). (C) Section parallel to tooth row, showing lamellar-walled duct (lwd) with osmiophlic substance in the lumen; relationships of central cells and chitin-secreting cells to tooth molds are also shown (scale bar = 8.0 μm). (D) Section parallel to tooth row, showing parts of Y-branching (arrowed) of a lamellar-walled duct; a salivary duct (s) also appears in oblique section (scale bar = 4.0 μm)

(Fig. 5 B) and appears to be extruded (Fig. 5 B: inset) between the epidermis and the mold. This creates an electron-dense layer, which appears granular in most preparations. These cells have RER just proximal to the surface, and a very few secretion granules are present in the cytoplasm. No Golgi apparatus has been seen, and Golgi bodies are not typical of chitin-secreting cells generally. The substance deposited against the tooth mold could be a cement to bond the siliceous tooth to the chitin which is deposited next. Several stages of chitin deposition are shown in Figs. 4 C and 8 A. Before silicification begins, the tooth mold becomes completely supported by chitin, except for the central cell attachment.

Prior to silicification, the tooth molds become attached to ducts reaching back to gland-shaped bodies in the base of the gnathobase (Figs. 2 B and 3 A). We believe these ducts are the unusual, electron-dense structures shown in Fig. 5 C and D, which we refer to as "lamellar-walled ducts". Because the gnathobase and these ducts are complexly curved, we have no section that traces the whole connection of mold to gland. We think the ovals of very dense material within the lamellar-walled ducts represent secretion in the lumen of the duct. The degree of elongation of this oval depends upon the obliquity of the cut. We have never observed this lumen to extend all the way to the tooth mold in any of many sections showing the dense lamellar structure. Probably we never obtained a section at precisely the right level. However, the lamellar bands extend to the surface of the epithelium between adjacent teeth (Fig. 5 C). They bifurcate there and attach to the edges of both tooth molds. All our preparations show large, apparently extracellular vacuoles beneath

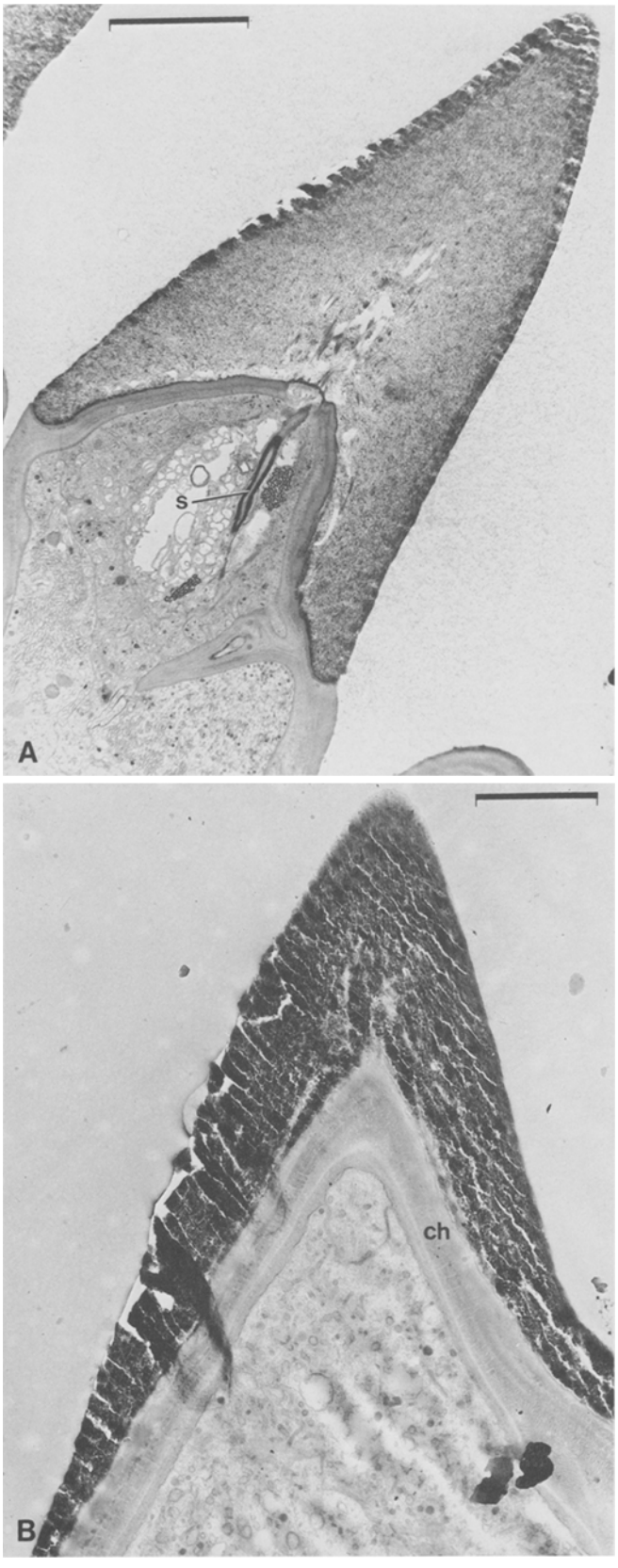

Fig. 6. *Calanus pacificus.* (A) Section perpendicular to tooth row, showing a tooth mold early in opal deposition stage; opal is laid down sequentially from distal surface to tooth base; section also shows passage of a salivary duct (s) adjacent to remains of central cell (scale bar = 6.0 μm). (B) Section showing fusion of a mature, fully silicified tooth to underlying chitin (ch) (scale bar = 2.6 μm)

this connection of the lamellar bands to the tooth molds. It is possible that the lumen does not extend to the mold proper, and that the lamellar structure itself conducts material in the most distal part of the route. None of our transverse sections below the tooth molds show the lamellar-walled ducts (Fig. 7 B, C, D). Probably all of the transverse sections were taken somewhat earlier in the development sequence and the lamellar-walled ducts either were not yet formed or were not yet strongly osmiophilic. Electron density of the lamellar duct walls varies among preparations. This may be intrinsic or an artifactual variation in osmium fixation. Between the dark lamellae there are numerous inclusions with smaller, transverse membranes within them. The inclusions appear to be mitochrondria, implying some energy demand for transport or for structural maintenance.

Silica deposition begins at the distal periphery of the mold (Fig. 6 A) and proceeds inward toward the base and center, until the entire mold is filled with opal that obscures the fibrous inclusions. In a mature tooth, the opal is tightly attached to the underlying chitin (Figs. 6 B and 7 A).

The tubular ducts continuous with passages through the teeth appear in TEM sections as electron-dense ovals and circles at all stages of development. A longitudinal section of a tubular duct in the apolysis space is shown in Fig. 4 A. Tubular duct trajectories pass in most cases just alongside the distal part of the central cell, through its connection to the tooth mold, through the mold, and into the apolysis space. In transverse sections below the central cell (Fig. 7 B and inset) the ducts are triangular, with extensions at each corner and sometimes from the sides also. These extensions must be flanges running along the corners of the triangular duct. Between these flanges are small cytoplasmic bands, bounded at the outer edge by cell membranes.

At its origin, the wall of the duct is attached to a basal body with a standard nine-filament pattern, shown in transverse section in Fig. 7 C. From this observation we postulate that the ducts are fused ciliary axonemes. They probably attach exocrine dermal glands, similar to those described by Doughtie and Ranga Rao (1979) from the gill of *Palaemonetes pugio*, to the pores in the opal teeth. Proximal to the basal bodies (Fig. 7 D), glandular reservoirs are seen in section. They have thin, electron-dense walls with small, evenly spaced extensions into the lumen, and are comparable to the locular complex in the hillock cell of the exocrine gland in the gill of *P. pugio*. Such glands have been reported from a variety of arthropods (e.g. cockroach dermal glands reported by Sreng and Quennedy 1976). Further work is needed for full description of these glands, but it seems certain that copepods are equipped to inject a secretion into their food during mastication.

Prior to full silicification, the folded chitin of the new exoskeleton (Fig. 3 B) is apparent in TEM sections (Fig. 8 A). These folds open at ecdysis to produce enlarged exoskeletal area. Coiled, electron-dense bodies (Fig. 8 B) are seen in the central cell of this phase; we have no idea of their significance.

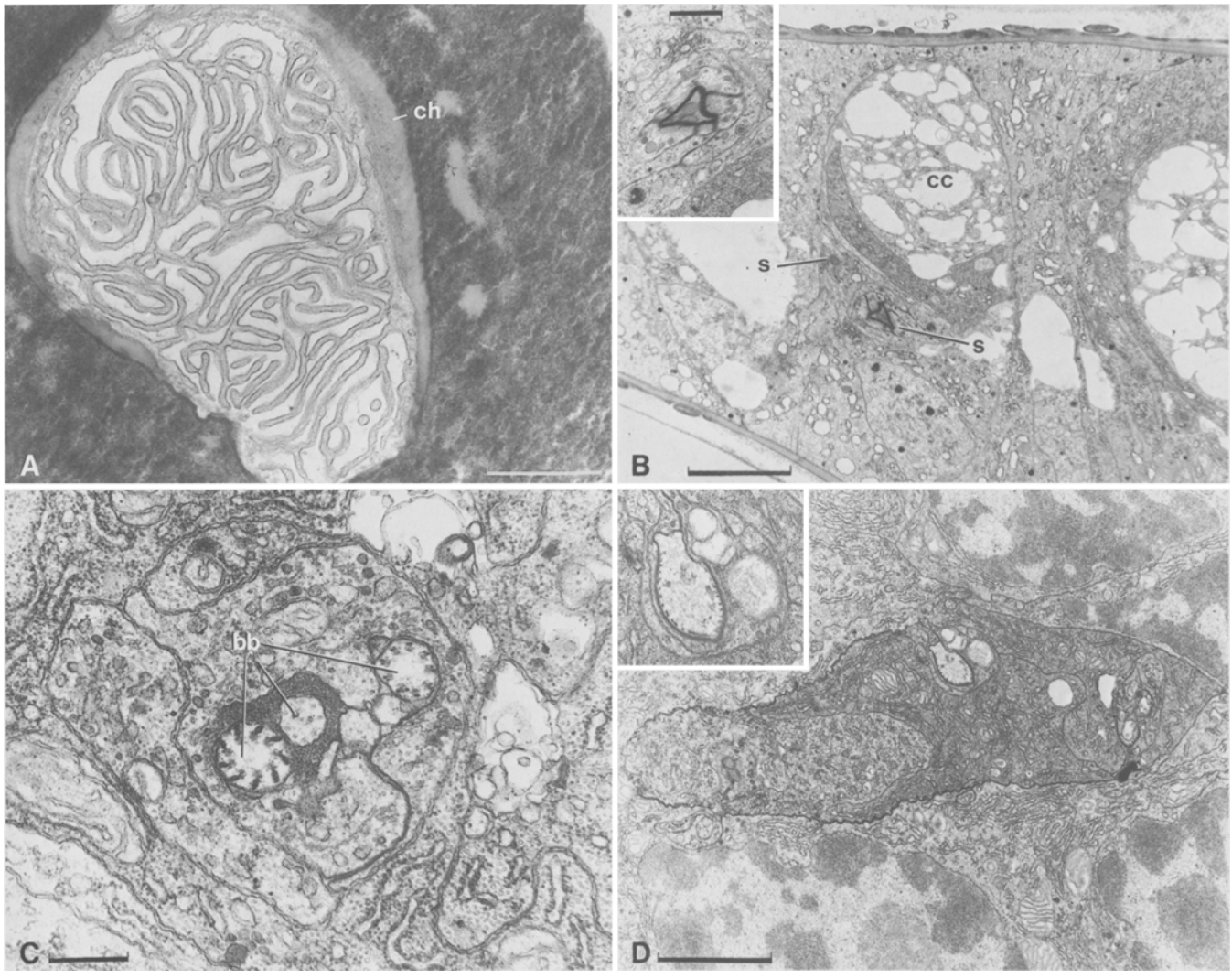

Fig. 7. *Calanus pacificus*. (A) Transverse section of a gnathobase at level of a new, fully silicified tooth, opal is closely fused to chitin (ch); central cell gap remains open, and folded lamellae of central cell are revealed as a complex labyrinth (scale bar = 1.0 μm). (B) Transverse section of gnathobase proximal to tooth molds; central cells (cc) of several teeth are shown; two salivary ducts (s) are shown in cross-section (scale bar = 4.0 μm); inset: detail of salivary duct (scale bar = 1.0 μm). (C) Transverse section proximal to (B); several basal bodies (bb) associated with salivary ducts are indicated (scale bar = 0.5 μm). (D) Transverse section proximal to (C), showing examples of locular complexes of salivary glands; note copious rough endoplasmic reticulum in surrounding cells (scale bar = 2.0 μm); inset: detail of locular chamber

Microprobe analysis

The microprobe produced counts over 200 s of electron-stimulated x-ray fluorescence emissions. After subtraction of small background counts from nearby chitin, chips of tooth in unstained sections gave the following proportions of elemental sources (according to x-ray energy) for emissions: silicon, 91.09%; copper, 4.18%; zinc, 4.83%. The full spectrum is shown in Fig. 9. Neither metal constituted as much as 4% of the atoms (of mass ≥ 18) in copepod teeth, since heavier elements produce proportionately more x-rays simply because of target size. We did not pursue a precise quantitative analysis. The absence of sulfur, whose emissions should fall on the energy scale between Si and Cu, implies that the protein content of the tooth is not particularly rich in cysteine or methionine. Electron diffraction images (not illustrated) from tooth chips in these sections were featureless, implying the amorphous structure of opal. A microprobe study was attempted for the lumen material of a silicification duct. However, it is impossible to find these in unstained sections. In stained sections, the osmium, uranyl and lead emissions would mask silicon emission. Such a study would not be impossible, but difficult.

Discussion

Opal structures occur in a variety of organisms including diatoms (elaborate tests), sponges (sculptured spicules), protozoans (various extruded surface plates and elaborate internal skeletons both occur), holothurians

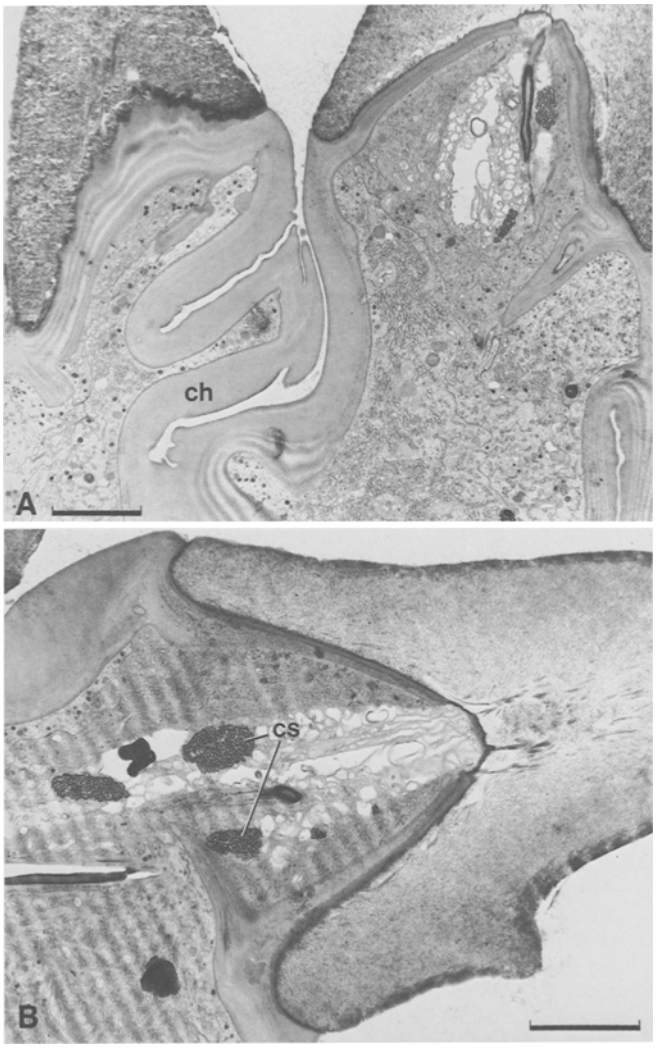

Fig. 8. *Calanus pacificus*. (A) Section, perpendicular to tooth row, of tooth molds during silicification; deep folding of new chitin (ch) shown between adjacent teeth (scale bar = 4.0 μm). (B) Section, perpendicular to tooth row, of a tooth during silicification; coiled structures (cs) in central cell are indicated (scale bar = 4.0 μm)

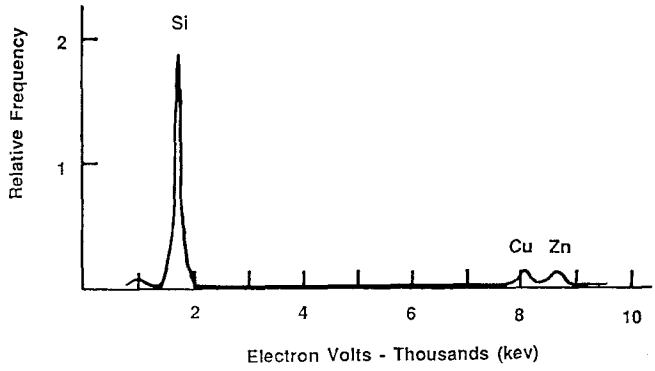

Fig. 9. *Calanus pacificus*. Energy dispersive X-ray fluorescence spectrum from sectioned chip of tooth. Section was of a gnathobase embedded in plastic without osmium fixation or staining. Peaks are identified by elemental symbols

(spicules), and vascular plants including equisitales, grasses ("phytoliths"), etc. In most cases the structures are formed intracellularly by a single cell type. Exceptions are copepod teeth and the opal radular base plates in patellid limpets (Runham et al. 1969, Lowenstam 1971, Mann et al. 1986). We could find no comprehensive study of the tissue structures involved in opal deposition by limpets, except that Mann et al. reported that a matrix of microfibers is involved, and they show this tooth matrix in section apposed to an epithelium. Study of this limpet structure is difficult because opal is deposited among crystals of goethite, an extremely hard, iron-oxide mineral, which are laid down first.

In copepods, the opal structure of the tooth and its attachment to the exoskeleton are formed by the coordinated, sequential activity of a number of functionally differentiated epithelial cells and a remote gland attached by a duct. The sequence of events in vertebrate tooth formation (e.g. Elwood and Bernstein 1968) is comparably complex, but even in that case, no remote glandular source of material for mineralization is involved. Occurrence of such a complex process in copepods alone among the Crustacea speaks for the length of their separate evolution.

While structurally more complex, tooth formation in copepods has some features in common with opal deposition in other animals. The presumably proteinaceous fiber mold is comparable to the protein fiber at the core of sponge spicules (Garrone 1968, Shore 1972, Simpson 1984). Amino acid or protein is also included at low concentrations in biogenic silica deposited into spaces between membranes without a protein-fiber core (diatoms, Sullivan and Volcani 1981; radiolarians, Anderson 1983). Apparently the protein fibers catalyze polymerization of silicic acid in their vicinity and this occurs in a variety of organisms, including copepods. While speculations on the chemistry of opal polymerization (reviewed by Degens 1976) usually invoke such a catalytic role, nothing specific is known about it. The absence of sulfur shown by our microprobe results for *Calanus pacificus* agrees with the data of Hecky et al. (1973), who showed that the amino acids in diatom walls and in the spicules of a siliceous sponge are low in sulfur-containing species.

Our finding of small but significant amounts of copper and zinc in tooth material suggests that these may play a role as cofactors in deposition. Zinc, in particular, forms the highly insoluble orthosilicate mineral willemite (solubility coefficient, $[Zn]^2[H_4SiO_4]/[H^+]^4 = 10^{-13.91}$; free energy of formation = −364 kcal/mol; Hem 1972), and the implied strong affinity for silicic acid may be part of the deposition mechanism. Willemite, *per se*, is not an important component because there is neither enough zinc nor any sign of crystalline structure. Grime et al. (1985) suggest that copper-containing oxidases may be involved in polymerization of aromatic amino acids into polyaromatic structures in the formation of siliceous deposits in the radular teeth of limpets. (The role of oxidases in sclerotization of molluscan radular tissues prior to silicification has been reviewed by Kerth 1983.) This, in conjunction with the statement of Mann et al. (1986) that silicic acid binds strongly to catechol-type molecules

(usually derivatives of tyrosine, a phenolic amino acid), may explain our observation of copper in copepod silica.

Copepods could provide a source of silica-associated protein for study, although considerable technical difficulties would be encountered. In particular, we found it very difficult to rear large numbers of specimens closely in phase with the molt cycle, which would be required in order to obtain substantial amounts of tooth-mold fiber at the stage prior to opal deposition. Possibly fiber useful for study of polymerization catalysis can be obtained from teeth by removal of old opal by basic solution or fluoride-etching.

While our figures illustrate the general structures involved in copepod tooth formation, there are many gaps. We did not study the fine structure of the silica-secreting gland. We have not fully elucidated the anatomy of the connections of the silicification ducts to the tooth molds. Further work is required before the full process, especially the actual transport and deposition of silica, can be described.

Our DIC photographs of *Neocalanus* spp. reveal that copepod teeth are equipped to deliver some sort of substance directly into newly broken food items through ducts opening immediately on the tooth surface. This substance could be either poisonous (to subdue active, animal prey) or an aid to digestion. Our micrographs reveal nothing of the nature of this material. The lumina of the exocrine dermal glands on the gills of *Palaemonetes pugio* also appear empty in the preparations of Doughtie and Ranga Rao (1979). Cahoon (1982) has shown that the mouth area of *Euchirella venusta* Giesbrecht secretes mucus which stains with Alcian Blue, specific for mucopolysaccharide. According to Cahoon's observations, *E. venusta* cases uneaten prey in this mucus, although it is not clear whether this copepod has a means to stay close to the resulting mucus balls once they are formed. Cahoon failed to find Alcian Blue reactions in the mouth area of other unspecified copepods. There is no reason to suppose that the gnathobase glands necessarily produce the mucus observed by Cahoon, since the labrum, labial palps and other parts of the mouth also contain many glands.

Thuesen et al. (1988) have shown that chaetognaths deliver paralyzing tetrodotoxin to their newly captured prey from pores in the mouth area. In copepods, the glands whose ducts open through the teeth may also deliver a toxin or sedative. Elaborate salivary secretions have been demonstrated in other arthropods, particularly in insects and ticks. Ishay (1972) reported "kinin-like" substances in the saliva of wasp larvae; prostaglandins playing a role in host/parasite relations have been found in cattle-tick saliva by Dickinson et al. (1976), Higgs et al. (1976), and Shemesh et al. (1979). Thus, other animals of structural complexity no greater than that of copepods have saliva with elaborate biochemical composition and function. Identification of the jaw and other oral secretions of copepods should be possible, if challenging, and will provide ecological insight.

Acknowledgements. This study was supported by the U.S. National Science Foundation, Grant OCE-7825762, with Oregon State University (OSU). The DIC work was performed at Ocean Research Institute (ORI), University of Tokyo, during the tenure of C. B. Miller as a visiting scientist. The Hitachi H500 scanning-transmission microscope was located at the Scripps Institution of Oceanography and was operated by E. Flentye. Many people helped, and we particularly thank E. Flentye, M. Nesson of OSU, and E. Thuesen of ORI.

Literature cited

Anderson, O. R. (1983). Radiolaria. Springer Verlag, New York

Beklemishev, K. V. (1954). The discovery of siliceous formations in the epidermis of lower Crustacea. Dokl. Akad. Nauk SSSR 97: 543–545

Beklemishev, K. B. (1959). On the anatomy of masticatory organs of Copepoda. Report 2: The masticatory edge in mandibles of certain species of Calanidae and Eucalanidae. Trudȳ Inst. Okeanol. 30: 148–155

Bocquet-Vendrine, J. (1979). La croissance tegumentaire et ses rapports avec la mue chez *Crinoniscus equitans* (crustace isopode cryptoniscien). Archs Zool. exp. gén. 120: 45–64

Cahoon, L. B. (1982). The use of mucus in feeding by the copepod *Euchirella venusta* Giesbrecht. Crustaceana 43: 202–204

Degens, E. T. (1976). Molecular mechanisms of carbonate, phosphate, and silica deposition in the living cell. Topics curr. Chem. (Inorg. Geochem.) 64: 1–112

Dickinson, R. G., O'Hagan, J. E., Schotz, M., Binnington, K. C., Hegarty, M. P. (1976). Prostaglandin in the saliva of the cattle tick *Boophilus microplus*. Aust. J. exp. Biol. med. Sci. 54: 475–486

Doughtie, D. G., Ranga Rao, K. (1979). Ultrastructure of an exocrine dermal gland in the gills of the grass shrimp, *Palaemonetes pugio*: occurrence of transitory ciliary axonemes associated with the sloughing and reformation of the ductule. J. Morph. 161: 281–307 (Doughtie misspelled "Dtughtie" in paper byline)

Drach, P., Tchernigovtzeff, C. (1967). Sur la methode de determination des stades d'intermue et son application generale aux crustaces. Vie Milieu 18: 595–607

Elwood, W., Bernstein, M. (1968). The ultrastructure of the enamel organ related to enamel formation. Am. J. Anat. 122: 73–94

Garrone, R. (1968). Collagene, spongine et squelette mineral chez l'eponge *Haliclona rosea* (O.S.) (Desmosponge, Haploscleride). J. Microscopie 8: 581–598

Grime, G. W., Watt, F., Mann, S., Perry, C. C., Webb, J., Williams, R. J. P. (1985). Biological applications of the Oxford scanning proton microprobe. Trends biochem. Sciences 10: 6–10

Hecky, R. E., Mopper, K., Kilham, P., Degens, E. T. (1973). The amino acid and sugar composition of diatom cell-walls. Mar. Biol. 19: 323–331

Hem, J. D. (1972). Chemistry and occurrence of cadmium and zinc in surface water and groundwater. Wat. Resour. Res. 8: 661–679

Higgs, G. A., Vane, J. R., Hart, R. J., Potter, C., Wilson, R. G. (1976). Prostaglandins in the saliva of the cattle tick, *Boophilus microplus* (Caststrini) (Acarina, Ixodidae). Bull. ent. Res. 66: 665–670

Ishay, J. (1972). Kinin-like substances in saliva of larvae of wasps and hornets. J. Pharm. Pharmac. 24: 747–748

Kerth, K. (1983). Radulaapparat und Radulabildung der Mollusken. II. Zahnbildung, Abbau und Radulawachstum. Zool. Jb. (Abt. Anat. Ont. Tiere) 110: 239–269

Lowenstam, H. A. (1971). Opal precipitation by marine gastropods (Mollusca). Science, N.Y. 171: 487–490

Mann, S., Perry, C. C., Webb, J., Luke, B., Williams, R. J. P. (1986). Structure, morphology, composition, and organization of biogenic minerals in limpet teeth. Proc. R. Soc. (Ser. B) 227: 179–190

Miller, C. B., Huntley, M. E., Brooks, E. R. (1984). Post-collection molting rates of planktonic, marine copepods: measurement, applications, problems. Limnol. Oceanogr. 29: 1274–1289

Miller, C. B., Nelson, D. M., Guillard, R. L., Woodward, B. L. (1980). Effects of media with low silicic acid concentration on tooth formation in *Acartia tonsa* Dana (Copepoda, Calanoida). Biol. Bull. mar. biol. Lab., Woods Hole 159: 349–363

Miller, C. B., Terazaki, M. (1989). The life histories of *Neocalanus flemingeri* and *Neocalanus plumchrus* in the Sea of Japan. Bull. Plankton Soc. Japan 36: 27–41

Mykles, D. L. (1980). The mechanism of fluid absorption at ecdysis in the American lobster. J. exp. Biol 84: 89–101

Runham, N. W., Thornton, P. R., Shaw, D. A., Wayte, R. C. (1969). The mineralization and hardness of the radular teeth of the limpet *Patella vulgata* L. Z. Zellforsch. 99: 608–626

Shemesh, M., Hadani, A., Shklar, A., Shore, L. S., Meleguir, F. (1979). Prostaglandins in the salivary glands and reproductive organs of *Hyalomma anatolicum excavatum* Koch (Acari: Ixodidae). Bull. ent. Res. 69: 381–385

Shore, R. E. (1972). Axial filament of siliceous sponge spicules, its organic components and synthesis. Biol. Bull. mar. biol. Lab., Woods Hole 143: 689–698

Simpson, T. L. (1984). The cell biology of sponges. Springer Verlag, New York

Skinner, D. M. (1985). Molting and regeneration. In: Bliss, D. E., Mantel, L. H. (eds.) The biology of Crustacea. Vol. 9. Integument, pigments, and hormonal processes. Academic Press, New York, p. 43–146

Sreng, L., Quennedy, A. (1976). Role of a temporary ciliary structure in the morphogenesis of insect glands. J. Ultrastruct. Res. 56: 78–95

Sullivan, B. K., Miller, C. B., Peterson, W. T., Soeldner, A. H. (1975). A scanning electron microscope study of the mandibular morphology of boreal copepods. Mar. Biol 30: 175–182

Sullivan, C. W., Volcani, B. E. (1981). Silicon in the cellular metabolism of diatoms. In: Simpson, T. L., Volcani, B. E. (eds.) Silicon and siliceous structures in biological systems. Springer Verlag, New York, p. 15–42

Thuesen, E. V., Kogure, K., Hashimoto, K., Nemoto, T. (1988). Poison arrowworms: a tetrodotoxin venom in the marine phylum Chaetognatha. J. exp. mar. Bio. Ecol. 116: 249–259